Received: 14 September 2020 | Accepted: 7 December 2021

DOI: 10.1111/poms.13656

POMS

SPECIAL ISSUE ARTICLE

Managing disease containment measures during a pandemic

Masoud Shahmanzari[1,2] | **Fehmi Tanrisever**[3] | **Enes Eryarsoy**[4] | **Ahmet Şensoy**[3]

[1] School of Business, Ozyegin University, Istanbul, Turkey

[2] Brunel Business School, Brunel University London, Uxbridge UB8 3PH, UK

[3] Faculty of Business Administration, Bilkent University, Ankara, Turkey

[4] Sabanci Business School, Sabanci University, Istanbul, Turkey

Correspondence
Fehmi Tanrisever, Faculty of Business Administration, Bilkent University, Ankara 06800, Turkey.
Email: tanrisever@bilkent.edu.tr

Handling editor: Special Issue Pandemic Editors

Abstract

Throughout the current COVID-19 pandemic, governments have implemented a variety of containment measures, ranging from hoping for herd immunity (which is essentially no containment) to mandating complete lockdown. On the one hand, containment measures reduce lives lost by limiting the disease spread and controlling the load on the healthcare system. On the other hand, such measures slow down economic activity, leading to lost jobs, economic stall, and societal disturbances, such as protests, civil disobedience, and increases in domestic violence. Hence, determining the right set of containment measures is a key social, economic, and political decision for policymakers. In this paper, we provide a model for dynamically managing the level of disease containment measures over the course of a pandemic. We determine the timing and level of containment measures to minimize the impact of a pandemic on economic activity and lives lost, subject to healthcare capacity and stochastic disease evolution dynamics. On the basis of practical evidence, we examine two common classes of containment policies—dynamic and static—and we find that dynamic policies are particularly valuable when the rate of disease spread is low, recovery takes longer, and the healthcare capacity is limited. Our work reveals a fundamental relationship between the structure of Pareto-efficient containment measures (in terms of lives lost and economic activity) and key disease and economic parameters such as disease infection rate, recovery rate, and healthcare capacity. We also analyze the impact of virus mutation and vaccination on containment decisions.

KEYWORDS
containment measures, COVID-19, optimization, pandemic, public policy

1 | INTRODUCTION

The outbreak of the novel coronavirus disease (COVID-19) in China in late December 2019 reminded us of the pandemics of recent history such as severe acute respiratory syndrome (SARS) and Middle East Respiratory Syndrome. Even though each pandemic has its own severity, mortality rate, and other specific disease characteristics, they share some similar economic consequences. At the time of writing this article, the number of people who have lost their lives worldwide due to the COVID-19 pandemic has exceeded 4,200,000,[1] the number of jobs lost in the United States has reached 22,200,000,[2] and expected GDP growth has been reduced by 10% in the United States and 12% in Europe (Gormsen & Koijen, 2020). Pandemics are far more than a health crisis; they also have significant economic and societal impacts.

Containing the spread of pandemics such as SARS and COVID-19 is a major challenge for governments due to economic, social, and political factors. During the COVID-19 pandemic, we have witnessed a wide range of containment measures. Some countries, such as Sweden, opted for a strategy of attempting to acquire herd immunity and adopted minimal containment measures. Other countries enacted strict containment measures, from imposing social distancing rules, closing schools and shopping malls, canceling arts and culture events, and closing borders to enforcing national lockdowns, curfews, and quarantines. The overarching goal of these measures is to slow the spread of the disease and flatten the pandemic's curve to bring it below the threshold of healthcare capacity. As illustrated in Figure 1, if the number of actively infected individuals exceeds the capacity of hospitals and clinical organizations at any given time, the quality

Accepted by Special Issue Pandemic Editors

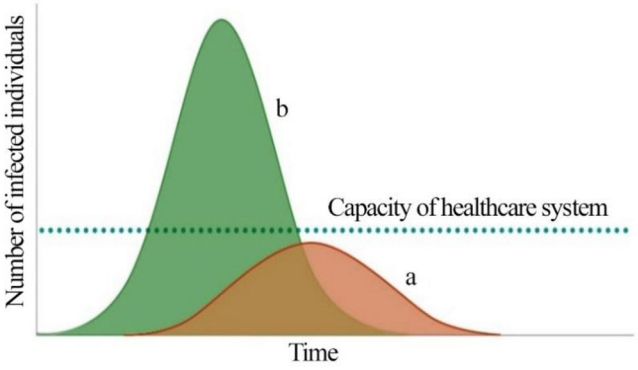

FIGURE 1 Two scenarios for the spread of pandemics with (a) and without (b) containment measures [Color figure can be viewed at wileyonlinelibrary.com]

of healthcare services will quickly degrade, leading to a significant increase in the number of deaths.

While imposing severe containment measures (e.g., curfews, large-scale social distancing, quarantine, and lockdowns) may limit the spread of the pandemic (as in the case of Australia) and decrease stress on the healthcare system, yet such severe measures may derail the economy by disrupting supply networks, manufacturing lines, and household demand for goods and services, leading to lost jobs, economic stall, and social disturbances. On the other hand, under mild or no containment measures, such as depending on herd immunity, the economic implications of the pandemic may be limited but the capacity of the healthcare system would be quickly exhausted, possibly leading to a significant amount of lives lost. Hence, when determining the severity of containment measures, governments face a stark trade-off between *maintaining economic activity* and *reducing lives lost*. In this study, we examine this trade-off by providing a multiobjective decision model that incorporates both the economic and health implications of containment measures into the decision maker's objective function.

Finding an appropriate containment policy is further complicated due to the unpredictable nature of disease spread and the impact of a government's other mediating actions during a pandemic. For example, the effectiveness of containment measures on the rate of disease spread can be uncertain due to unpredictable social reactions to the measures, possible virus mutation, and potential vaccination and treatment development. Economic stimulus packages and short-term investments into healthcare may also condition the impact of government containment measures on economic activity and lives lost. Finally, the impact of measures may also be moderated by the level of economic and containment measures taken by the rest of the world, because a global economic slowdown will eventually affect local economies. Our model aims to incorporate these relevant problem dynamics into a unified decision-making framework for governments.

Given the duration of a typical pandemic (2–3 years), we track the economic impact of the disease through the change in the industrial production (IP) index,[3] which is a good proxy for change in gross domestic product (GDP). Estimating the sensitivities of the economic activity level and disease spread to the strictness (level) of containment measures is a key driver of our decision model. Hence, in Section 5, we provide two empirical models to estimate those sensitivities. We use University of Oxford's (2020) country-level containment reports for tracking the level of containment measures and calculate the disease spread again at the country level using publicly reported case numbers. University of Oxford reports an aggregate containment level for countries, which can be scaled between 0 and 1, where 0 means no containment effort and 1 means complete lockdown. The details of the empirical models used for estimating the input parameters are provided in Section 5.

In this paper, we develop a stochastic multiobjective dynamic program to determine the level and timing of government interventions during a pandemic. The dual objectives of the hypothetical government are to (i) minimize the impact of containment measures on economic activity (measured as change in IP) and (ii) minimize the expected number of lives lost during the pandemic, subject to the stochastic evolution dynamics of the disease over time and the capacity of the healthcare system. Motivated by real-life containment activities, we focus on deriving and analyzing two common classes of control policies: (i) static containment policies, where the level of containment measures remains mostly fixed throughout the planning horizon, and (ii) dynamic/flexible containment policies, where the level of containment measures is revised based on the evolution of disease spread over time. For example, the herd immunity approach in Sweden and the full lockdown in China during the early phases of the pandemic can be classified as examples of static containment policies. It is also possible to consider static containment policies, where the containment level is raised to a specific threshold between no containment and full lockdown, and is kept fixed throughout the planning horizon. Dynamic containment policies are also commonly used in practice. For example, the United Kingdom started with a low level of containment by imposing loose social distancing rules in early April 2020, then, as infections increased, it raised the containment level by imposing additional measures, and finally, in September 2020, the country moved to a full lockdown for 2 weeks. When cases decreased by early winter, they eased the lockdown restrictions.

Although it is intuitive that dynamic containment policies would perform better than static policies due to their flexibility in responding to a pandemic's evolution, it is not a priori evident whether these benefits are significant enough to justify the switching costs associated with frequently updating containment measures. Frequently updating containment measures are not desirable as they are subject to significant tangible and intangible economic, social, and political costs. In addition to the deadweight economic losses due to opening and closing businesses, frequently changing the level of containment during the pandemic creates economic and social uncertainty, which may lead to prolonged labor disturbances and social instability. In this paper, we focus on the quantifiable benefits of dynamic policies (over static policies), which

can be compared to the costs of implementing such complex rules in practice.

We contribute to the literature with the following main points:

- We provide a decision-support framework for policymakers by integrating disease-spread models with stochastic dynamic optimization techniques. Unlike the existing research on pandemic disease control, we examine the broader problem of managing a government's level of containment measures to prevent the spread of a pandemic while minimizing the effect of such measures on economic activity and lives lost. Our model reflects the decision maker's ability to revise containment measures as the disease evolves over time.
- Our framework enables us to characterize a Pareto-efficient set of containment policies that are undominated in terms of lives lost and level of economic activity. Through a comprehensive set of sensitivity analyses, we examine the impact of healthcare capacity and disease characteristics on containment decisions. We find that under the Pareto-optimal set of containment policies, multiple peaks in the pandemic are likely to occur unless when the disease spread rate is high and the recovery period is long. In addition, targeting a high level of economic activity typically generates fewer but steeper peaks in the pandemic.
- We compare static and dynamic containment policies and observe that the dynamic policies are most beneficial when the disease spread is low and recovery takes longer. Further, governments targeting a moderate level of economic activity benefit more from dynamic policies.
- In addition, a close examination of the Pareto-optimal set of containment policies reveals a key insight: Under low or high levels of containment measures, lives lost are highly sensitive to target economic activity level. Under intermediate levels of containment measures, however, changes in target economic activity level do not significantly affect lives lost.
- Finally, we also analyze the impacts of possible vaccination and virus mutation on the Pareto-optimal set of containment measures and disease spread. We find that under a relatively low level of target economic activity, starting vaccinations after 9 months effectively flatten the peaks in a pandemic. If vaccinations are delayed, the benefits in terms of reduced lives lost quickly decrease. We also observe that the effectiveness of vaccination programs (in terms of reduced lives lost) is significantly compromised under high levels of target economic activity. Virus mutation has a qualitatively similar, but opposite, effect on the results.

The rest of the paper is structured as follows: We provide a review of the related literature in Section 2, followed by a description of our time-dependent disease spread model in Section 3, and the decision model in Section 4. In Section 5, we discuss the estimation of the model parameters, and we devote Section 6 to the analysis of the model. We conclude with discussions and future research directions in Section 7. In addition, in Supporting Information Appendices A and B, we discuss extending our results under vaccination and virus mutation scenarios. Finally, we provide the details of our empirical analysis in Supporting Information Appendix C.

2 | LITERATURE REVIEW

In the literature, there is an extensive amount of research on modeling pandemic-spread dynamics using approaches that range from deterministic models (e.g., Albi et al., 2021; Chen et al., 2016; Sene, 2020) to stochastic models, such as discrete event simulation and system dynamics (Ghaffarzadegan & Rahmandad, 2020; Xie, 2020), to hybrid models (Ardabili et al., 2020; Funk et al., 2018). However, there is limited work linking outbreak dynamics to decision-support models. With a few notable exceptions (Boloori & Saghafian, 2020; Eryarsoy et al., 2022), the relevant literature mostly focuses on analyzing pandemic spread.

Recently, a number of studies have been published exploring different types of containment measures to control the spread of a pandemic. Many of these studies examine the impact of a particular containment action—such as air traffic restrictions (Zlojutro et al., 2019), complete lockdown (Singh & Adhikari, 2020), and social distancing (Qiu et al., 2020; Thunström et al., 2020)—on the disease spread. Having focused on the COVID-19 case, a comprehensive study by Ferguson et al. (2020) evaluates the impact of nonpharmaceutical interventions, including case isolation at home, voluntary home quarantine, social distancing of elderly people, closures of schools and universities, and general-population social distancing. The authors conclude that to significantly reduce contact rates, multiple interventions need to be integrated. Giordano et al. (2020) suggest a forecasting model based on a modified version of Kermack–McKendrick's susceptible, infected, recovered (SIR) model to plan effective pandemic control. Using a compartmental model, the authors discriminate between diagnosed and undiagnosed patients and run scenario analyses for implementing countermeasures. Similar to Ferguson et al. (2020), their findings reveal that multiple intervention policies, such as widespread testing, contact tracing, and social distancing, should be integrated to end the outbreak. The literature also considers the impact of mobility patterns (Delen et al., 2020), age-specific contact settings (Kyrychko et al., 2020), as well as popular discontent and social fatigue on pandemic control policies (Ouardighi et al., 2021).

A few recent works examine the economic impact of intervention policies for COVID-19. For instance, Boloori and Saghafian (2020) provide an analytical decision-making framework based on a compartmental disease-spread model to study the economic burdens of pandemic containment policies in the United States. They suggest that while severe societal intervention policies may not be cost effective, the policies imposed by the US government over a 4-month period increased quality-adjusted life years per capita. In

another attempt, Eryarsoy et al. (2022) develop deterministic mathematical formulations to study the economic impact of government interventions. The authors develop a multistart variable neighborhood search algorithm to suggest intervention strategies for policymakers. Their findings reveal that when disease severity is low and the estimated economic burden of pandemic containment policies is high, the policymaker should not engage in any intervention policy.

The societal value placed on lowering the statistical likelihood of one death is referred to as the value of statistical life (VSL) (Viscusi & Aldy, 2003). While various methods of fixing a monetary value for a human life have already been suggested by different protagonists, pandemics forced the globe to confront yet another unsettling trade-off between human life/misery and economic gain. Within labor-market studies, a sizable body of research has emerged that estimates VSL (Mrozek & Taylor, 2002). In healthcare operations, this issue is usually addressed from the "efficiency" point of view (Harris, 1987). As a result, to enable comparisons across different areas of healthcare, standard measures of health outcome, such as the quality-adjusted life years (QALY) (Zeckhauser & Shepard, 1976) and disability-adjusted life years (DALY) (Murray, 1994), were suggested. While the debate on the theoretical underpinnings and practical implications of those measures are still ongoing, the common overarching goal is to identify a healthcare strategy that results in a minimal cost per QALY or DALY (Whitehead & Ali, 2010). When considering a particular treatment for a particular illness, such as a cardiovascular disease or diabetes mellitus, QALY and DALY provide good measures of the cost-effectiveness of a treatment in terms of allocating financial resources. In a pandemic context, however, the number of lives lost provides an easier and direct way of measuring the effectiveness of containment policies. Hence, we focus on the number of lives lost as one of the governmental objectives in our context.

In this study, we aim to provide a decision support framework for policymakers by integrating disease-spread models with dynamic optimization models. Unlike the existing research, we examine the broader problem of optimizing a government's level of containment measures to prevent the spread of a pandemic while considering the dual objectives of minimizing lives lost and maximizing level of economic activity. Our analysis uncovers the connection between these two critical objectives by providing a Pareto-optimal set (efficient frontier) of containment policies. Hence, our multiobjective approach is a generalization of the constrained optimization models, which minimize lives lost (or maximize QALY) under a given level of economic activity or budget constraint. Moreover, we estimate the model parameters through a comprehensive empirical analysis, which provides strong practical implications. We numerically illustrate the impact of healthcare capacity and other mediating factors on the trade-off between lives lost and economic activity during a pandemic. We also identify the factors that drive multiple peaks in a pandemic under the Pareto-optimal set of policies.

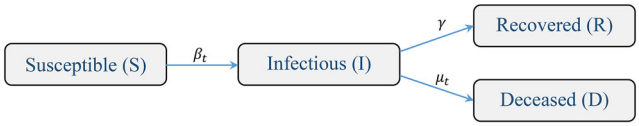

FIGURE 2 The time-varying SIRD framework and its parameters [Color figure can be viewed at wileyonlinelibrary.com]

3 | PANDEMIC MODEL

In the literature, there are several approaches for modeling disease spread. Perhaps the simplest and most well known is Kermack–McKendrick model, also known as the SIR model. SIR is a Markov model that has been used to explain the fast increase and decrease in the number of infected individuals in many pandemics. The SIR and its variants (such as susceptible-infected-susceptible (SIS), and susceptible-exposed-infectious-recovered (SEIR)) generally fall under deterministic compartment models, and have been widely used to analyze the spread of pandemic diseases (Keeling & Rohani, 2011; Wearing et al., 2005; Wu et al., 2020). These models are represented by a set of differential equations, where various disease-specific parameters describe the growth rates of disease among population compartments (Hethcote, 2000).

As illustrated in Figure 2, in this study we use a modified version of the SIR model. Our susceptible-infected-recovered-deceased (SIRD) model consists of four compartments (or states) and three parameters, where the transition between states is indicated by arrows. The state variables s_t, i_t, r_t, and d_t, respectively, denote the susceptible, infected, recovered, and deceased number of individuals at time t. Parameter β_t is the infection rate (i.e., the expected number of individuals an infected person will pass the infection on to at each time period) and parameter γ describes the recovery rate. The recovery rate can be numerically estimated by studying the virus or through data analysis. For example, for COVID-19, if the average duration of a reported case until recovery is 14 days, γ may be estimated roughly as 1/14 per day. The infection rate β_t (infections/time), on the other hand, depends on two factors: (i) transmissibility of the disease (infections/contact) or transmissibility per contact and (ii) contacts per time unit. While the former factor depends on the type of disease, the latter can be managed by a government's containment measures. We model β_t as a derived decision variable (which can be partially influenced by containment measures) and γ as a disease-specific constant.[4] The parameter μ_t is the state-dependent death rate, which is explained in Section 4. The modified version of the SIR model used in our study is provided in Equation (1):

$$\begin{aligned} s_{t+1} - s_t &= -\beta_t s_t i_t \\ i_{t+1} - i_t &= \beta_t s_t i_t - \gamma i_t - \mu_t i_t \\ r_{t+1} - r_t &= \gamma i_t \\ d_{t+1} - d_t &= \mu_t i_t \end{aligned} \tag{1}$$

We note that in the medium and long term, a government's healthcare-related measures (such as investing in drug and treatment development as well as increasing ICU capacity) may affect the recovery rate γ and spread of the disease. It is possible to extend our model by partially endogenizing γ, but we believe this will only have a second-order effect given the time frame of a pandemic and investment lead times. Hence, we focus on controlling β_t in this study.

It is worth noting that the SEIR model (with state variables Susceptible, Exposed but not infectious (E), Infectious, and Recovered) may also be used to model the spread of COVID-19 because there is a period where the infected individual does not show any symptoms but is capable of infecting others. Having a very similar structure to SIRD, the SEIR model consists of only one additional parameter, λ, which manages the transition from the state "exposed" to "infectious." We also conducted our main analysis with a SEIR model and obtained materially the same insights.

4 | OPTIMIZATION MODEL

In this section, we provide a multi-period discrete-time optimal control problem to determine the level and timing of a government's containment measures during a pandemic. We use discrete weekly intervals both for modeling disease spread and making containment decisions. In each decision period t, the government decides the level of containment measures $m_t \in [0, 1]$. Our definition of m_t is based on the Oxford Government Stringency Index C (University of Oxford, 2020), which categorizes government containment and closure actions during a pandemic into eight subgroups: school closures, workplace closures, cancelation of public events, restrictions on gathering size, public transport closures, stay-at-home requirements, restrictions on internal movement, and restrictions on international travel. The severity of the actions in each group is measured on a simple scale of severity/intensity, and then these values are scaled and combined to obtain a single containment index between 0 and 1. In our work, we use this aggregate containment measure definition to model our decision variables.

Higher values of m_t imply stricter containment measures. For practical purposes, the level of m_t can be interpreted as follows: (i) $m_t = 0$ means implementing no measures (such as adopting a herd immunity approach); (ii) $m_t \in (0,\ 0.3]$ means imposing low-level measures (such as calling for voluntary social distancing rules, requiring the use of masks, etc.); (iii) $m_t \in (0.3,\ 0.7]$ corresponds to medium-level measures (such as imposing partial curfews, canceling social events and gatherings, etc.); and (iv) $m_t \in (0.7,\ 1]$ can be interpreted as high-level measures (such as imposing national lockdown and large-scale quarantines as well as shutting down nonessential supply chains). In our model, the containment level m_t conditions both the level of economic activity and the spread of disease and hence the number of lives lost. We provide our mathematical model and notation in Table 1.

4.1 | Mathematical formulation

We assume that the government has two objectives without any a priori preference for one of them. The first objective is to minimize the impact of containment measures on economic activity, as defined in the following:

Objective 1. *Minimize the impact of containment measures on expected level of economic activity* (*i.e., maximize the expected level of economic activity*)

$$\max: \frac{1}{T}\sum_{t=1}^{T} E_{\tilde{\epsilon}_{IP}} IP_t\left(\vec{\boldsymbol{m}}_{\boldsymbol{t}}; c_{IP}, \tilde{\epsilon}_{IP}\right), \tag{2}$$

where the function $IP_t(\vec{\boldsymbol{m}}_{\boldsymbol{t}}; c_{IP}, \tilde{\epsilon}_{IP})$ is the IP index (a common proxy for level of economic activity) in period t, as a function of the vector of containment measures $\vec{\boldsymbol{m}}_{\boldsymbol{t}}$, control variables c_{IP}, and a random shock $\tilde{\epsilon}_{IP}$.[5] In Section 5, we empirically estimate the parameters of this function and discuss the control variables c_{IP} in detail. We normalize the initial level of economic activity at $t = 0$ to $IP_0 = 100\%$ and formulate our objective to maximize the average expected level of IP index over the planning horizon as given by $\frac{1}{T}\sum_{t=1}^{T} E_{\tilde{\epsilon}_{IP}} IP_t(\vec{\boldsymbol{m}}_{\boldsymbol{t}}; c_{IP}, \tilde{\epsilon}_{IP})$. The expectation is taken over the independent and identically distributed random shock $\tilde{\epsilon}_{IP}$ in each period. The second objective of the government is to minimize the expected number of lives lost during the pandemic, as defined in the following:

Objective 2. *Minimize the total number of expected lives lost*

$$\min: \sum_{t=1}^{T} E_{\tilde{\epsilon}_\beta} l_t\left(\vec{\boldsymbol{v}}_{\boldsymbol{t}}, \vec{\boldsymbol{m}}_{\boldsymbol{t}}; \tilde{\epsilon}_\beta\right), \tag{3}$$

where

$$l_t(\vec{\boldsymbol{v}}_{\boldsymbol{t}}, \vec{\boldsymbol{m}}_{\boldsymbol{t}}; \tilde{\epsilon}_\beta) = \mu_{t+1} i_{t+1} \tag{4}$$

and

$$\mu_{t+1} = \begin{cases} \rho_L & \text{if } \rho_H i_{t+1}/H \le UC \\ \hat{\rho}_L & \text{if } \rho_H i_{t+1}/H > UC \end{cases} \tag{5}$$

The function $l_t(\vec{\boldsymbol{v}}_{\boldsymbol{t}}, \vec{\boldsymbol{m}}_{\boldsymbol{t}}; \tilde{\epsilon}_\beta)$gives the number of lives lost given the current state of the disease $\vec{\boldsymbol{v}}_{\boldsymbol{t}} = [s_t, i_t, \mu_t, \beta_{t-1}]$, the vector of past and current containment measures $\vec{\boldsymbol{m}}_{\boldsymbol{t}} = [m_1, \ldots, m_t]$, and a random shock $\tilde{\epsilon}_\beta$, which represents the uncertain evolution of disease spread.[6] In Section 5, we empirically estimate the change in disease infection rate $\Delta\beta_t(\vec{\boldsymbol{m}}_{\boldsymbol{t}}; \tilde{\epsilon}_\beta)$ as a function of the vector of containment measures $\vec{\boldsymbol{m}}_{\boldsymbol{t}}$. In period t, the change in infection rate $\Delta\beta_t(\vec{\boldsymbol{m}}_{\boldsymbol{t}}; \tilde{\epsilon}_\beta)$

TABLE 1 Notation for the mathematical model

Sets and indices	t, $\mathbf{T}$	Time period and set of time periods for the model, $\mathbf{T} = \{1, \dots, \mathbf{T}-1\}$
Parameters	S_0, I_0, R_0, and D_0	Number of susceptible, infected, recovered, and deceased individuals, respectively, at $t = 0$
	N	Population size (normalized to 1)
	H	Normalized healthcare capacity in terms of ICUs
	UC	Critical utilization level of healthcare capacity
	γ and β_0	Recovery rate and base infection rate of the disease, respectively
	ρ_H	Hospitalized fraction of infected individuals
	ρ_L and $\hat{\rho}_L$	Deceased fraction of infected individuals when the utilization of healthcare capacity is below UC and above UC, respectively
Decision variable	m_t	$m_t \in [0,\ 1]$, level of containment measures in period $t \in \mathbf{T}$. We denote the vector of containment measures up to period t by $\vec{\boldsymbol{m}}_{\boldsymbol{t}} = [m_1, \dots, m_t]$. We define $m_0 = 0$ and $\vec{\boldsymbol{m}}_{\boldsymbol{0}} = [m_0]$.
Derived variables	s_t	Number of susceptible individuals in period $t \in \mathbf{T}$
	i_t	Number of infected individuals (active cases) in period $t \in \mathbf{T}$
	r_t	Number of recovered individuals in period $t \in \mathbf{T}$
	d_t	Number of deceased individuals in period $t \in \mathbf{T}$
	μ_t	Death rate in period $t \in \mathbf{T}$
	β_t	Infection rate in period $t \in \mathbf{T}$
	$\Delta\beta_t(\vec{\boldsymbol{m}}_{\boldsymbol{t}}; \tilde{\epsilon}_\beta)$	Change in infection rate in period $t \in \mathbf{T}$, as a function of containment decisions $\vec{\boldsymbol{m}}_{\boldsymbol{t}}$ and a random shock $\tilde{\epsilon}_\beta$, such that $\beta_t = \beta_{t-1} + \Delta\beta_t(\vec{\boldsymbol{m}}_{\boldsymbol{t}}; \tilde{\epsilon}_\beta)$
	$IP_t(\vec{\boldsymbol{m}}_{\boldsymbol{t}}; c_{IP}, \tilde{\epsilon}_{IP})$	Level of economic activity in period $t \in \mathbf{T}$, as a function of containment decisions $\vec{\boldsymbol{m}}_{\boldsymbol{t}}$, control variables c_{IP},[1] and a random shock $\tilde{\epsilon}_{IP}$
	$\vec{\boldsymbol{v}}_{\boldsymbol{t}}$	$\vec{\boldsymbol{v}}_{\boldsymbol{t}} = [s_t, i_t, \mu_t, \beta_{t-1}]$, vector of state variables defining the state of the disease in period $t \in \mathbf{T}$

[a]The variable c_{IP} denotes the significant control variables of the empirical estimation model used to estimate the relationship between the IP index and containment measures in Section 5.1.

together with the current state of the disease $\vec{\boldsymbol{v}}_{\boldsymbol{t}}$ determine the number of infected individuals i_{t+1}. Accordingly, the utilization of the healthcare system is given by $\rho_H i_{t+1}/H$, where H is the normalized healthcare capacity (in number of ICUs) and ρ_H is the hospitalized fraction of infected individuals.

In addition to the inherent disease characteristics, utilization of the healthcare system affects the quality of treatment and the death rate, μ_{t+1}, due to infection. In particular, we assume that if utilization of the healthcare system is lower than a critical level UC, then ρ_L percentage of infected individuals lose their lives. If utilization exceeds UC, then the death rate increases to $\hat{\rho}_L > \rho_L$.

We use the scalarization method to represent our multiobjective, multiperiod stochastic dynamic program. Scalarizing a multiobjective problem means formulating a single-objective version of the problem using a scalar $\alpha \in [0, 1]$, such that the Pareto-optimal solutions of the original problem can be obtained by solving the scalarized problem under different values of the scalar α. It is important to note that with scalarization, we do not define weights or priorities for objectives, but rather, scalarization provides a parameterized problem to identify Pareto-optimal solutions. For more details and other approaches for modeling and solving multi-objective problems (such as the hybrid method, elastic constraint method, and ε-constraint method), see Chapter 3 in Ehrgott (2005):

$$V_{t,\alpha}\left(\vec{\boldsymbol{v}}_{\boldsymbol{t}}; \vec{\boldsymbol{m}}_{\boldsymbol{t-1}}\right) = \max_{m_t \in [0,1]} \left\{ \alpha \frac{E_{\tilde{\epsilon}_{IP}} IP_t\left(\vec{\boldsymbol{m}}_{\boldsymbol{t}}; c_{IP}, \tilde{\epsilon}_{IP}\right)}{T} + (1-\alpha) E_{\tilde{\epsilon}_\beta} l_t(\vec{\boldsymbol{v}}_{\boldsymbol{t}}, \vec{\boldsymbol{m}}_{\boldsymbol{t}}; \tilde{\epsilon}_\beta) + E_{\tilde{\epsilon}_{IP}, \tilde{\epsilon}_\beta} V_{t+1,\alpha}(\vec{\boldsymbol{v}}_{\boldsymbol{t+1}}; \vec{\boldsymbol{m}}_{\boldsymbol{t}}) \right\}, \text{ s.t.,} \tag{6}$$

$$s_1 = S_0, \quad i_1 = I_0, \quad r_1 = R_0, \quad d_1 = D_0, \tag{7}$$

$$s_{t+1} - s_t = -\beta_t s_t i_t, \quad \forall t \in \mathbf{T}, \tag{8}$$

$$i_{t+1} - i_t = \beta_t s_t i_t - \gamma i_t - \mu_t i_t, \quad \forall t \in \mathbf{T}, \tag{9}$$

$$r_{t+1} - r_t = \gamma i_t, \quad \forall t \in \mathbf{T}, \tag{10}$$

$$d_{t+1} - d_t = \mu_t i_t, \quad \forall t \in \mathbf{T}, \tag{11}$$

$$\mu_{t+1} = \begin{cases} \rho_L & \text{if } \rho_H i_{t+1}/H \le UC \\ \hat{\rho}_L & \text{if } \rho_H i_{t+1}/H > UC \end{cases}, \quad \forall t \in \mathbf{T}, \tag{12}$$

$$\beta_t = \beta_{t-1} + \Delta\beta_t\left(\vec{\boldsymbol{m}}_t; \tilde{\varepsilon}_\beta\right), \quad \forall t \in \mathbf{T}, \tag{13}$$

$$V_{T,\alpha}\left(\vec{\boldsymbol{v}}_T; \vec{\boldsymbol{m}}_{T-1}\right) = \left\{ \alpha \frac{E_{\tilde{\varepsilon}_{IP}} IP_T\left(\vec{\boldsymbol{m}}_T; c_{IP}, \tilde{\varepsilon}_{IP}\right)}{T} + (1-\alpha) E_{\tilde{\varepsilon}_\beta} l_T\left(\vec{\boldsymbol{v}}_T, \vec{\boldsymbol{m}}_T; \tilde{\varepsilon}_\beta\right) | m_T = 0 \right\}, \tag{14}$$

At time t, given the state of the disease $\vec{\boldsymbol{v}}_t$ and the vector of previous containment decisions $\vec{\boldsymbol{m}}_{t-1}$, the government decides the current level of containment m_t. The first two terms of the objective function $\{\alpha \frac{E_{\tilde{\varepsilon}_{IP}} IP_t(\vec{\boldsymbol{m}}_t; c_{IP}, \tilde{\varepsilon}_{IP})}{T} + (1-\alpha) E_{\tilde{\varepsilon}_\beta} l_t(\vec{\boldsymbol{v}}_t, \vec{\boldsymbol{m}}_t; \tilde{\varepsilon}_\beta)\}$ denote the expected immediate effect of containment measures on economic activity and lives lost in the current period, under a given scalarization parameter α. The second term of the objective is the cost-to-go function.

Together with the initial conditions in Equation (7), Equations (8)–(12) describe the modified time-varying SIRD model for the spread of the disease over time (i.e., s_t, i_t, r_t, and d_t indicate the number of susceptible, infected, recovered, and deceased individuals in period t). Equation (13) describes the relationship between the infection rate β_t and the vector of containment measures $\vec{\boldsymbol{m}}_t$. Finally, Equation (14) specifies the termination condition. Given the long pandemic planning horizon in practice, our particular choice of termination condition has no significant effect on the results.

The model in (6)–(14) is a high-dimensional dynamic program with a nonconvex feasible region.[7] As a result, even when we discretize the problem with monthly decision epochs, the model is still computationally intractable given that a pandemic may last for more than 1 year. Therefore, we continue with a weekly model to update disease evolution and containment measures and resort to heuristic containment policies. Next, we explain our parameter estimations for our model.

5 | PARAMETER ESTIMATION

In this section, we provide a brief empirical analysis to determine the sensitivities of the economic activity level IP_t and disease spread rate β_t to the level of containment measures $\vec{\boldsymbol{m}}_t$. In particular, we aim to estimate the coefficients of the percentage change in economic activity level and the change in disease spread rate. The results of the empirical estimations are fed to the optimization model (given by Equations 6–14) when determining the level and timing of government containment measures.

5.1 | Estimating the impact of containment measures on economic activity

During the COVID-19 outbreak, evaluating the impact of a government's containment measures on economic activity has been challenging due to the short time span of the evaluation period combined with the low dissemination frequency of the main macroeconomic variables. In order to examine the impact of governments' containment measures on economic activity, we first set our sample country selection to G20 members. According to the International Monetary Fund (IMF), G20 countries account for 80% of global economic productivity, and therefore are considered a good representative of the world's total production output. However, since the European Union (EU) is counted in the G20, together with its largest economies of Germany, France, the United Kingdom, and Italy, we remove the EU from our sample set. Further, another member, Saudi Arabia, prefers not to disclose its various statistics on macroeconomy and international trade. Therefore, we also exclude it from our analysis.

Change in level of economic activity is commonly measured by change in GDP. However, in our case, GDP cannot be taken as the dependent variable, because due to its quarterly announcement frequency it gives us an exceedingly small sample to make a robust inference about statistical analysis. Moreover, initial GDP announcements are usually revised multiple times throughout the year, making them even more questionable to use in our analysis.

As a higher frequency proxy for GDP, we take the seasonally adjusted IP index, which is announced on a monthly basis. One of the main reasons why IP is a good proxy for GDP is that value added by IP represents a substantial share of GDP, especially for big economies such as G20 members (see NBER's Business Cycle Dating Committee[8]; Rünstler & Sédillot, 2003). However, some G20 members do not disclose their IP values or stopped disclosing them some time ago. These countries are Australia, Argentina, India, Indonesia, Mexico, and South Africa, and so we exclude them from our sample country set. Eventually, we end up with 12 countries: the United States (1), China (2), Japan (3), Germany (4), the United Kingdom (6), France (7), Italy (8), Brazil (9), Canada (10), Russia (11), Korea (12), and Turkey (19), where the numbers in the parentheses denote the countries' positions in the nominal GDP ranking in the world at the end of year 2019 by IMF estimates. The resulting country sample accounts for more than 65% of global GDP in the same year.[9] The details of the empirical analysis and data are provided in Appendix C in the Supporting Information.

5.1.1 | Dependent variable

The monthly IP values cover from the end of December 2019 till the end of May 2020 (June 2020) for Brazil, Canada,

Germany, France, the United Kingdom, Italy, Russia, and Turkey (for China, Japan, Korea, and the United States). Since we consider the monthly changes in IP values as the dependent variable, we end up with 64 country × month observations in an unbalanced panel data format. Accordingly, our *dependent variable* $g_{t,y}$ is the percentage change in IP in month t for country y, that is,

$$g_{t,y} = \frac{(IP_{t,y} - IP_{t-1,y})}{IP_{t-1,y}}. \quad (15)$$

5.1.2 | Main independent variable

In our setup, the independent variable of special interest is a government's level of containment measures. Suppose that the *independent variable* $m_{t,y} \in [0, 1]$ denotes the level of government containment measures in month t for country y. In our dataset, this variable ranges from no containment ($m_{t,y} = 0$) to total lockdown ($m_{t,y} = 1$) over time across the countries. For example, when COVID-19 was formally announced as a pandemic, Sweden and the United Kingdom took almost no containment measures for a few months while Italy and Spain quickly moved to full containment and lockdown. As a proxy for this variable, we use Oxford's Government Stringency Index C (University of Oxford, 2020). As explained in the Introduction, this index categorizes government containment and closure actions during the pandemic into eight subgroups, measures the severity/intensity of each action, and then combines these values to form a single aggregate containment index between 0 and 1.

This index is weekly updated, whereas our IP variable is a monthly indicator. Therefore, we synchronize these two datasets by taking only the monthly changes in Oxford's index. In our empirical analysis, we consider the monthly level change (index-level difference between two consecutive months) as the key independent variable:

$$\Delta m_{t,y} = m_{t,y} - m_{t-1,y} \quad (16)$$

However, since measures taken by a government in the previous period can also affect the current period's IP, we include both the current ($\Delta m_{t,y}$) and lagged ($\Delta m_{t-1,y}$) values of this variable in our model (we experimented with other lagged containment variables and found that they had no significant impact; see Appendix C in the Supporting Information).

5.1.3 | Control variables

We also included a number of control variables that would likely condition the impact of a government's containment measures on economic activity. In particular, we included the monthly change in the variables described in Table 2.[10]

5.1.4 | Model and results

We estimate the following model in the form of an unbalanced panel regression to measure the impact of government containment and closure actions:

$$g_{t,y} = a + b_1\Delta m_{t,y} + b_2\Delta m_{t-1,y} + b_3\Delta e_{t,y} + b_4\Delta om_{t,y} + b_5\Delta om_{t-1,y} + b_6\Delta oe_{t,y} + \varepsilon_{t,y} \quad (17)$$

To have a robust framework, we use three alternative panel regression models, namely (i) pooled estimation, (ii) fixed-effect estimation, and (iii) random effects (generalized least square) estimation, where standard errors are heteroscedasticity and autocorrelation robust. We observe that the model performs a fairly good fit to the data with an R^2 value around 0.50 for all estimation methods. Both quantitative and qualitative results are similar across the alternative estimation techniques, and therefore we interpret the economic findings based on the pooled regression results provided in Table 3. We observe that $\Delta m_{t,y}$, $\Delta m_{t-1,y}$, and $\Delta om_{t-1,y}$ are the only significant variables. In particular, a 0.1-point increase in a country's stringency index decreases its IP by 1.62% in the current month and 1.68% in the following month. Moreover, as hypothesized, the weighted stringency index of the major trading partners also has a negative effect on a country's IP. According to our estimates, a 0.1-point increase in the trade partners' stringency index dampens the IP of that country by 2.43% in the following month. A more detailed description of the models and discussion of the empirical results are available in Appendix C in the Supporting Information.

On the basis of our empirical analysis, we use the significant variables and their coefficients in Table 3 to describe the relationship between containment measures and the level of IP index, that is, given IP_{t-1}, the IP index in period t, $IP_t(\vec{\boldsymbol{m}}_t; c_{IP}, \tilde{\varepsilon}_{IP})$, in the optimization model is specified such that $\vec{\boldsymbol{m}}_t = [m_{t-2}, m_{t-1}, m_t]$ and the control variable c_{IP} is Δom_{t-1}. For expositional clarity, we present our numerical analysis in Section 6 for the case when the value of the control variable is set to zero.

5.2 | Estimating the sensitivity of containment measures on disease spread

In this part, we examine the effect of a government's level of containment measures on the infection rate of the disease, that is, we estimate $\Delta\beta_t(\vec{\boldsymbol{m}}_t; \tilde{\varepsilon}_\beta)$. At this stage, our main dependent variable is $\Delta\beta_{t,y} = \beta_{t,y} - \beta_{t-1,y}$, that is, the change in infection rate in period t for country y, whereas the independent variables are $\Delta m_{t,y}, \Delta m_{t-1,y}, \ldots, \Delta m_{t-4,y}$, that is, the change in the level of a government's containment measures in periods $t, t-1, \ldots, t-4$, respectively, for country y (we experimented with further lagged containment variables; however, we found that estimations produce unreasonable findings mostly due to the noise arising from including many

TABLE 2 Explanation of control variables

Control variable	Description	Justification	Data
$\Delta e_{t,y}$	Change in economic countermeasures taken by country y in month t to mitigate the negative economic impact of pandemic	While containment measures are expected to decrease the economic activity in a country, economic stimulus packages such as furlough support and shared work programs may help businesses increase output	Oxford's Government Economic Response Index E
$\Delta om_{t,y}$ $\Delta om_{t-1,y}$	Change in average weighted level of containment measures taken by the 10 largest trade partners in months t and $t-1$ for country y	Containment measures taken by major economic partners may have a dampening effect on bilateral international trade through diminished export/import activities	Oxford's Government Stringency Index C, and TradeMap database
$\Delta oe_{t,y}$	Change in average weighted level of economic countermeasures taken by the 10 largest trade partners in month t for country y	Although containment measures taken by trading partners are expected to decrease the export/import volumes between these countries, economic stimulus packages provided by trading partner countries may stimulate international trade	Oxford's Government Economic Response Index E, and TradeMap database

TABLE 3 Pooled estimation results for the impact of containment measures on economic activity

Pooled estimation	Coefficient	*t*-stat	*p*-Value
$\Delta m_{t,y}$	−0.162	−1.89	0.06*
$\Delta m_{t-1,y}$	−0.168	−2.23	0.03**
$\Delta e_{t,y}$	−0.092	−1.23	0.23
$\Delta om_{t,y}$	0.097	0.54	0.60
$\Delta om_{t-1,y}$	−0.243	−2.33	0.02**
$\Delta oe_{t,y}$	0.017	0.09	0.93

$R^2 = 0.501$

TABLE 4 Pooled estimation results for the impact of containment measures on disease spread

Pooled estimation	Coefficient	*t*-stat	*p*-Value
$\Delta m_{t,y}$	−0.0723	−5.50	0.000***
$\Delta m_{t-1,y}$	−0.0587	−4.47	0.000***
$\Delta m_{t-2,y}$	−0.0375	−2.85	0.004***
$\Delta m_{t-3,y}$	−0.0284	−2.20	0.028**
$\Delta m_{t-4,y}$	−0.0202	−1.81	0.070*

$R^2 = 0.0201$

lags). We expect that containment measures have a lagged negative effect on the infection rate. As in Section 5.1, we use Oxford's Government Stringency Index C as a proxy for the level of containment measures.

In our setup, both $\beta_{t,y}$ and $m_{t,y}$ are available weekly, therefore we proceed by working on the weekly observations for an enriched sample. The time frame for the estimations is from March 20, 2020 to January 29, 2021, giving us 46 weeks in total. We consider all countries that have data on both infection rate and containment measures, which totals 87 countries, encompassing more than 90% of the global population. Overall, we utilize $87 \times 46 = 4002$ country × week observations in a balanced panel structure. To analyze the impact of containment measures on the infection rate, we run the following empirical model:

$$\Delta\beta_{t,y} = c_1\Delta m_{t,y} + c_2\Delta m_{t-1,y} + \cdots + c_5\Delta m_{t-4,y} + \varepsilon_{t,y} \quad (18)$$

For robustness, we use three alternative models, namely (i) pooled estimation, (ii) fixed-effect estimation, and (iii) random effects (generalized least square) estimation. Since all models yield similar results, we only report the coefficients obtained via pooled estimation.

According to the estimation results, the current and past 4 weeks' containment measures taken by a government can significantly reduce the disease infection rate in that country, which confirms our earlier expectations. Table 4 also shows that the impact of containment measures on infection rate is gradually recognized over time. Based on our empirical analysis, we use the significant variables and their coefficients in Table 4 to describe the relationship between containment measures and the change in disease spread, that is, $\Delta\beta_t(\vec{\boldsymbol{m}}_t; \tilde{\varepsilon}_\beta)$ is specified such that $\vec{\boldsymbol{m}}_t = [m_{t-5}, \ldots, m_{t-1}, m_t]$.

5.3 | SIRD model estimates and numerical setup

Our disease-spread model includes two key parameters: recovery rate γ and base infection rate β_0, that is, the natural rate of disease infection in the absence of any containment measures. Without loss of generality, $1/\gamma$ consequently corresponds to the recovery period of the infectious disease. In the case of COVID-19, this duration ranges from 5 to 30 days (in severe cases). Following the extant literature on COVID-19, we take the average duration of recovery to be 14 days, which corresponds to a recovery rate of $\gamma = 1/14$. For sensitivity analysis, we consider three levels of average recovery duration, such that $1/\gamma = \{7, 14, 21\}$, where 14 days denotes the base-case scenario.

Regarding the base infection rate β_0 of the disease, a range of figures from 0.1 to 0.56 is reported in the literature (Roques et al., 2020; Sanche et al., 2020;

Sugishita et al., 2020; Tang et al., 2020; Trilla, 2020).[11] The fluctuations in base infection rates are driven by a number of causes, including treatment quality and social differences across countries as well as increasing public awareness about the disease. Virus mutation, which we model in Appendix B in the Supporting Information, also directly impacts infection rate.[12] For our base-case scenario, we set $\beta_0 = 0.25$ and conduct our analysis for the range $\beta_0 = \{0.2, 0.25, 0.3\}$. We set the variance of the random shocks $\tilde{\epsilon}_\beta$ and $\tilde{\epsilon}_{IP}$ low enough to avoid negative parameters and reduce the computational time needed to achieve a sufficiently low level of statistical variability in our results. In our numerical experiments, we assume that $\tilde{\epsilon}_\beta$ follows a normal distribution with mean 0 and standard deviation 0.001, and the variance of $\tilde{\epsilon}_{IP}$ is set to zero.

For COVID-19, the hospitalized fraction of individuals ρ_H ranges between 0.7% and 4% of reported cases (Ritchie et al., 2020). Given the above-mentioned studies, we posit that the reason for this variation may be due to testing and reporting differences as well as country-specific healthcare practices. For our numerical study, we set $\rho_H = 2\%$. To account for the increased case fatality rate when the healthcare resources are saturated, we introduce ρ_L and $\hat{\rho}_L$: fatality rate of individuals when the utilization of healthcare capacity is below a critical level UC and above UC, respectively. We let $UC = 1$. Based on the COVID-19 data, we set $\rho_L = 0.5\%$ and consider three levels of $\hat{\rho}_L$, such that $\hat{\rho}_L \in \{1.2\rho_L, 1.4\rho_L, 1.6\rho_L\}$. Regarding healthcare capacity, we assume 10 ICU units per 100,000 people (after normalization, this number corresponds to $H = 0.0001$ in our model) and run a sensitivity analysis for three levels of H, such that $H \in \{0.00008, 0.0001, 0.00012\}$. Finally, we consider a planning horizon of 700 days.

6 | ANALYSIS: CONTAINMENT POLICIES

The high dimensionality and nonconvexity of the dynamic program in Equations (6)–(14) render it impossible to optimally solve real-sized problems. Therefore, motivated by our practical observations, we focus on two common classes of control policies: (i) *static containment policies* and (ii) *dynamic containment policies*. We use the infectious ratio, $u_t = i_t s_t$, to trigger changes in the level of containment actions, which provides a good measure of the speed of disease spread at a given time t. First, we consider static containment policies, such that a government initiates a fixed containment level m_S once the infectious ratio u_t reaches a certain threshold Q_{tr}. After containment measures are put in place, they are kept fixed until the end of the planning horizon unless the infectious ratio becomes very close to zero. Obviously, countries may revise their containment levels over time as the infectious ratio fluctuates in response to the development of the pandemic and containment measures. We will explore those dynamic policies in Section 6.2.

6.1 | Static containment policies

Static containment policies may be desirable by governments due to their simplicity and the provided certainty about planning future social and economic activities. Canceling work meetings and travel plans in response to a change in containment measures would have both economic and social consequences. Similarly, frequently opening and closing a business, as a result of changes in containment levels, may result in deadweight hiring and layoff costs. Similar deadweight losses also apply when negotiating rents and financial contracts in the markets. In addition, from a societal point of view, uncertainty associated with containment measures may lead to social disturbances and instability. In this sense, implementing a static containment policy provides individuals and businesses with more certainty about the level of containment measures, enabling them to avoid deadweight social and economic costs due to cancellations and updates, but these policies have limited flexibility to respond to the evolution of the pandemic.

During the COVID-19 pandemic, we have observed examples of static policies in China and Sweden. China triggered a full containment policy in Wuhan soon after infection numbers reached a certain threshold and kept those strict containment measures in place until the infection numbers significantly decreased. Sweden adopted a static policy to the other extreme. After infection numbers reached a certain level in the country, they initiated loose voluntary social distancing and mask use and they have mostly kept these measures fixed throughout the pandemic.

The generalized version of the static policies discussed above is given in Equation (19). Here, Q_{tr} denotes an initial policy trigger, such that if the infectious ratio u_t exceeds Q_{tr}, then the containment level is raised to a static level of m_S and kept fixed until u_t falls significantly below that initial trigger. The parameter $\theta > 1$ describes the exit strategy, that is, if the infectious ratio falls below Q_{tr}/θ after the implementation of measures, the decision maker sets $m_t = 0$ and lifts the measures. We observe that θ ranges from 2 to 5 in practice based on COVID-19 data. In our experiments, we set $\theta = 2$:

$$\begin{aligned} &\text{if } u_t \geq Q_{tr} &&: m_t = m_S, \quad \forall t \in \mathbf{T} \\ &\text{if } Q_{tr}/\theta \leq u_t < Q_{tr} &&: \begin{cases} m_t = m_S | m_{t-1} \neq 0 \\ m_t = 0 | m_{t-1} = 0 \end{cases}, \quad \forall t \in \mathbf{T}. \\ &\text{if } 0 \leq u_t < Q_{tr}/\theta &&: m_t = 0, \quad \forall t \in \mathbf{T} \end{aligned} \tag{19}$$

In practice, it is not possible to initiate a containment measure as soon as the first person gets infected by a disease. It takes a certain amount of time and effort for governments to detect and verify the significance of an infection and for the World Health Organization to determine the importance and severity of the situation. On the basis of COVID-19 experience, we will take this threshold to be $Q_{tr}^{\min} = 0.00086\%$, that is, during COVID-19, most countries began to initiate containment measures after infectious ratio u_t reached

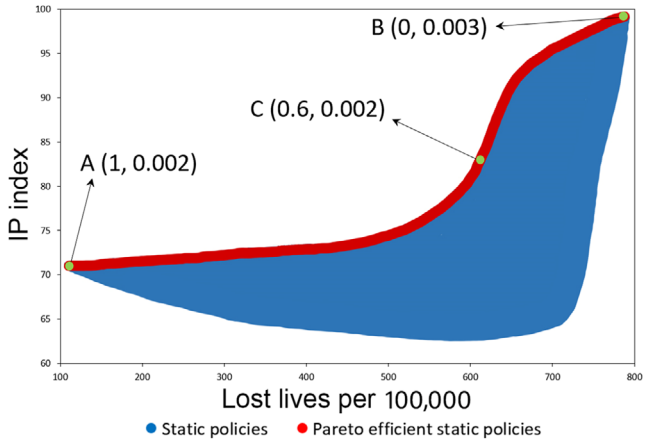

FIGURE 3 Feasible and Pareto-efficient static policies with minimum intervention trigger $Q_{tr}^{\min} = 0.00086\%$ and $\theta = 2$ [Color figure can be viewed at wileyonlinelibrary.com]

0.00086%.[13] Hence, we restrict our static policy search to $Q_{tr} > Q_{tr}^{\min}$. Figure 3 illustrates the results of the static policy in terms of the decision maker's dual objectives. Unless otherwise stated, all analyses are conducted under the base-case parameter setting, as described in Section 5.3.

In Figure 3, each point corresponds to a particular static policy identified by the pair of containment level and policy trigger (m_S, Q_{tr}). For each point, the x-axis provides the number of lives lost per 100,000 people, and the y-axis shows the level of economic activity (average IP index) during the planning horizon. In the figure, the line formed by the red points provides the Pareto-efficient set of static policies (efficient frontier), such that the policies in this set are undominated among the feasible static policies. The efficient frontier in Figure 3 illustrates the trade-off between lives lost and economic activity under static policies. Point A at the bottom left corresponds to a full lockdown ($m_S = 1$, $Q_{tr} = 0.002$), point B at the top right denotes a herd immunity approach ($m_S = 0$, $Q_{tr} = 0.003$), and for illustrative purposes, we present an intermediate case on the efficient frontier with point C ($m_S = 0.6$, $Q_{tr} = 0.002$) in the middle. Under herd immunity, as expected, the impact on economic activity is minimal yet a relatively large number of lives are lost. The full lockdown is the opposite case, with the fewest number of lives lost yet the highest impact on economic activity. We note that the containment level decreases along the efficient frontier as we move from point A to B.

The shape of the efficient frontier in Figure 3 reveals an important relationship (which also persists under the dynamic policies) between the level of economic activity and lives lost during the pandemic. For low and high levels of IP index, the number of lives lost is highly sensitive to changes in economic activity, whereas this sensitivity decreases under intermediate levels of IP index. For example, increasing the level of economic activity from 75% to 80% results in 78 additional lives lost, whereas increasing economic activity from 80% to 85% results in fewer than 35 additional lives lost. A close examination of this result together with the structure of containment policies on the efficient frontier reveals a key managerial insight: Under low or high economic activity targets, containment has a marginal impact on economic activity but has a significant influence on lives lost. However, when economic activity targets are set at intermediate levels, the number of lives lost becomes less sensitive to variations in containment level.

Static policies are desirable due to their stable nature and predictability in practice. However, they lack the flexibility to react to changes in infection numbers. Next, we discuss another class of common policies, which dynamically revises containment level based on disease spread, and compare it with static policies.

6.2 | Dynamic containment policies: Band control policies

Band-type dynamic containment policies are commonly used by governments. In this case, when the infectious ratio u_t reaches a certain threshold, the government initiates a set of containment actions that are kept in place for as long as the infectious ratio stays within certain bounds, that is, within a band. When the infectious ratio exceeds the bounds of the current containment measures (in either direction), the containment measures are revised accordingly and again kept fixed for as long as u_t stays within a new band.

In practice, most governments' dynamic policies resemble single- and double-band policies, and hence we only focus on such policies. Equation (20) formalizes a single-band control policy, and Figure 4 provides a visual illustration of it for the base-case parameters:

$$\begin{aligned}
&\text{If } u_t \geq Q_2 && : m_t = m_H, \quad \forall t \in \mathbf{T} \\
&\text{If } Q_1 \leq u_t < Q_2 && : \begin{cases} m_t = m_H | m_{t-1} = m_H \\ m_t = m_L | m_{t-1} \neq m_H \end{cases}, \quad \forall t \in \mathbf{T} \\
&\text{If } Q_1/\theta \leq u_t < Q_1 && : \begin{cases} m_t = m_L | m_{t-1} \neq 0 \\ m_t = 0 | m_{t-1} = 0 \end{cases}, \quad \forall t \in \mathbf{T} \\
&\text{If } 0 \leq u_t < Q_1/\theta && : m_t = 0, \quad \forall t \in \mathbf{T}
\end{aligned}$$

$$\text{such that } Q_1 < Q_2 \text{ and } m_L < m_H. \tag{20}$$

The single-band policy is described by a control band (Q_1, Q_2) and a containment level pair (m_L, m_H). That is, when the infectious ratio u_t first exceeds the lower bound of the band Q_1, the containment level is raised to m_L and stays at this level unless u_t exceeds the upper bound Q_2 or falls below the exit threshold Q_1/θ. If the infectious ratio u_t exceeds the upper bound of the band Q_2, the containment level is raised to m_H and is kept at that level as long as u_t remains above the lower bound of the band, that is, $Q_1 \leq u_t$.

Figure 4 illustrates implementing an arbitrary single-band policy with parameters $(Q_1 = 0.05, Q_2 = 0.1)$ and $(m_L = 0.2, m_H = 0.8)$. The figure shows the level of containment measures m_t, number of infected i_t, and infectious ratio u_t over time. We also present the number of infected under herd immunity as a comparison. The band policy effectively caps

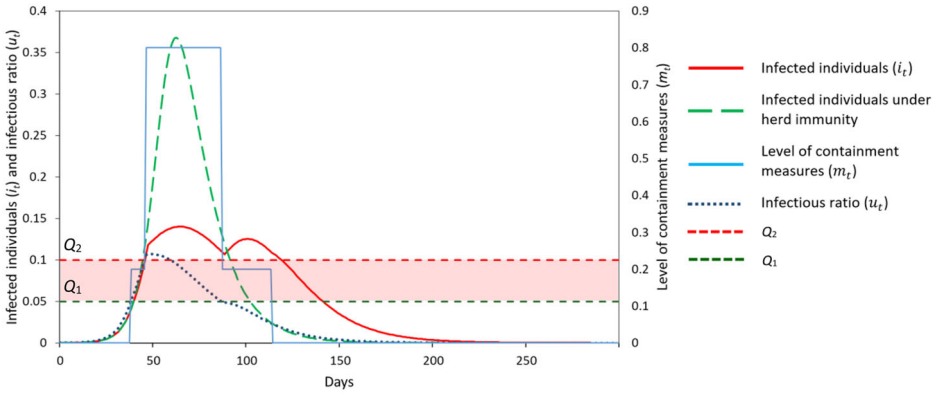

FIGURE 4 Illustration of a single-band policy [Color figure can be viewed at wileyonlinelibrary.com]

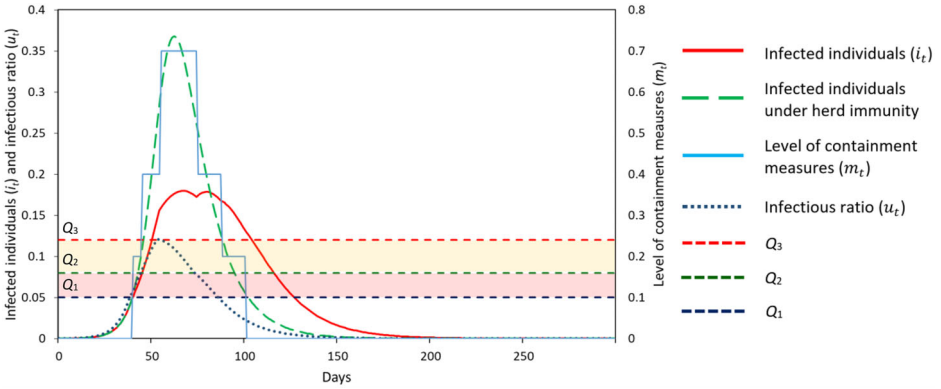

FIGURE 5 Illustration of a double-band policy [Color figure can be viewed at wileyonlinelibrary.com]

the peak of the pandemic and spreads it over a longer period of time as compared to herd immunity. As illustrated in Figure 4, band containment policies lift containment measures with a lag as the infectious ratio starts to decrease. This policy structure is in line with our practical observations during COVID-19 that most governments are more cautious in lifting measures as compared to imposing them. Next, we discuss the double-band policy, which is formalized in Equation (21):

$$
\begin{aligned}
&\text{If } u_t \geq Q_3 && : m_t = m_H, \quad \forall t \in \mathbf{T}\\
&\text{If } Q_2 \leq u_t < Q_3 && : \begin{cases} m_t = m_H | m_{t-1} = m_H \\ m_t = m_M | m_{t-1} \neq m_H \end{cases}, \quad \forall t \in \mathbf{T}\\
&\text{If } Q_1 \leq u_t < Q_2 && : \begin{cases} m_t = m_M | m_{t-1} = m_M \text{ or } m_H \\ m_t = m_L | m_{t-1} = m_L \text{ or } 0 \end{cases}, \quad \forall t \in \mathbf{T}\\
&\text{If } Q_1/\theta \leq u_t < Q_1 && : \begin{cases} m_t = m_L | m_{t-1} \neq 0 \\ m_t = 0 | m_{t-1} = 0 \end{cases}, \quad \forall t \in \mathbf{T}\\
&\text{If } 0 \leq u_t < Q_1/\theta && : m_t = 0, \quad \forall t \in \mathbf{T}\\
&\text{such that } Q_1 < Q_2 < Q_3 \text{ and } m_L < m_M < m_H.
\end{aligned}
\tag{21}
$$

Figure 5 depicts implementing an arbitrary double-band policy with parameters ($Q_1 = 0.05, Q_2 = 0.08, Q_3 = 0.12$) and ($m_L = 0.2, m_M = 0.4, m_H = 0.7$). Simply, a double-band policy is a generalization of a single-band policy. It is described by two control bands, given by the pairs (Q_1, Q_2) and (m_L, m_M), and (Q_2, Q_3) and (m_M, m_H). Based on the infectious ratio u_t, the policy determines the level of containment similar to the single-band case, except that now there are two nested control bands. Next, to compare static and dynamic policies, we numerically determine the Pareto-efficient set of dynamic policies.

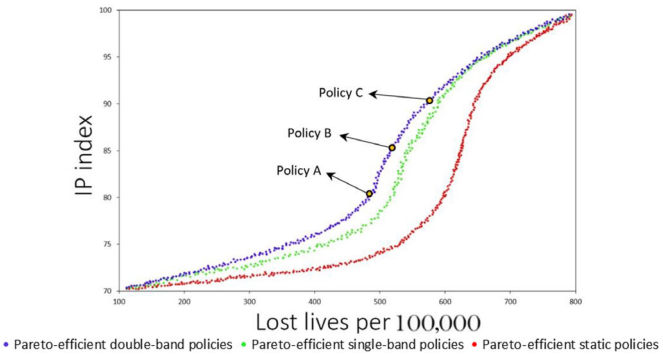

FIGURE 6 Pareto-efficient set of static, single-, and double-band policies *Note*: In our numerical illustrations, we report infection numbers and infectious ratios with daily intervals for better granularity [Color figure can be viewed at wileyonlinelibrary.com]

Figure 6 illustrates the Pareto-efficient set of static and dynamic policies under our base-case parameter setting,

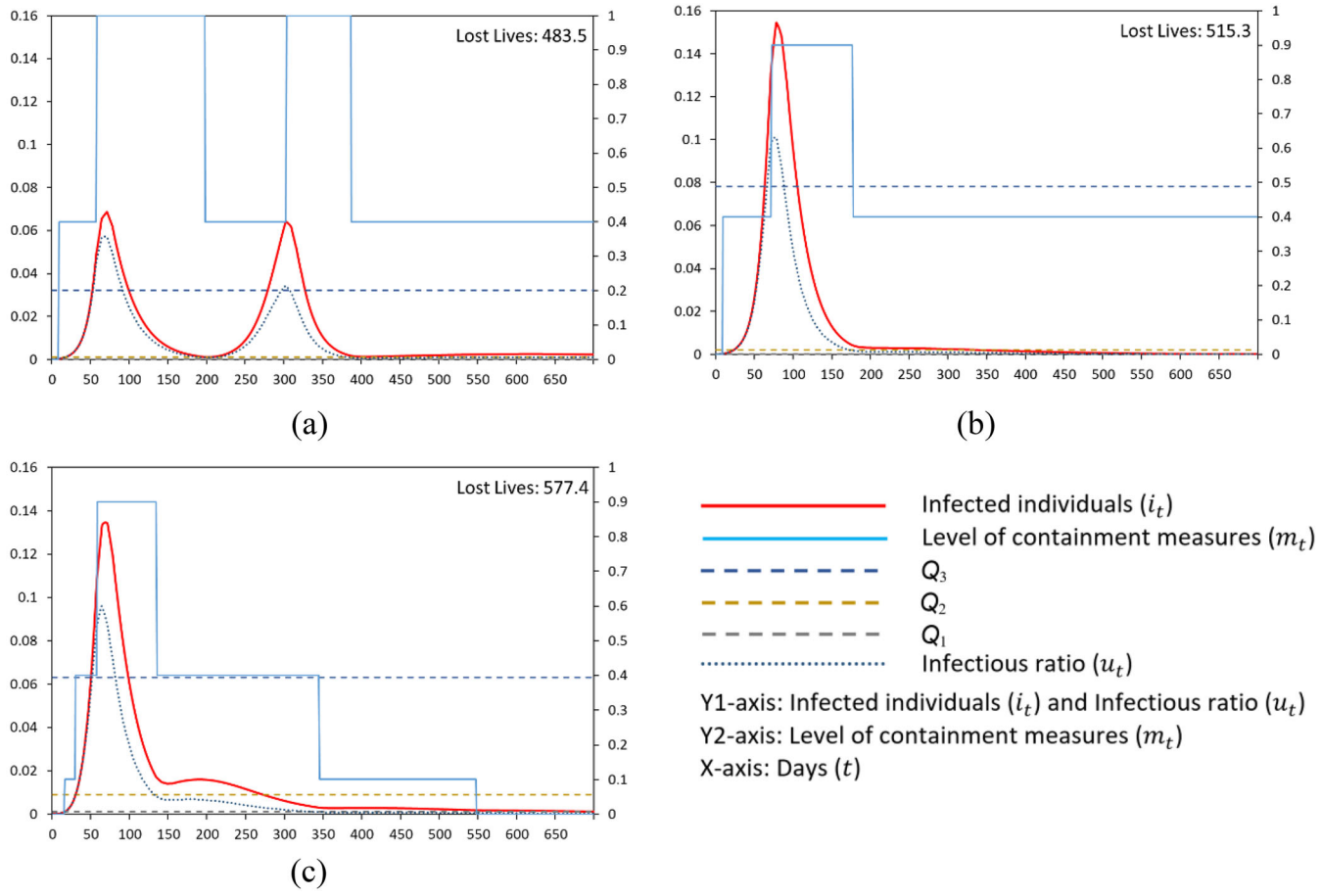

FIGURE 7 Containment measures and infected individuals over time under the Pareto-efficient double-band policies with IP index = (a) 80%, policy A; (b) 85%, policy B; and (c) 90%, policy C. *Note*: In Figure 7a,b, the threshold Q_1 is too low to be observed visually [Color figure can be viewed at wileyonlinelibrary.com]

where the upper, middle, and lower lines represent Pareto-efficient double-band, single-band, and static policies, respectively. We observe that there can be a significant gap between the performance of static and dynamic policies. Moreover, double-band policies outperform single-band policies as well. After two bands, considering more control bands has little value in our model, and hence we focus on double-band policies for the rest of our numerical analysis when referring to dynamic containment policies.

In Figure 7, we examine the performance of three Pareto-efficient double-band containment policies such that the level of economic activity corresponds to 80% (policy A), 85% (policy B), and 90% (policy C). Figure 7a shows the performance of policy A, which generates 483.5 lives lost per 100,000 individuals. The policy results in two peaks in the pandemic. It initiates a low level of intervention at the beginning of the pandemic, followed by a strict containment after day 56; once the infectious ratio decreases substantially around day 203, the policy decreases the containment level, and the number of active cases starts to increase again, resulting in a second peak around day 301, followed by another short period of strict containment. After day 385, the government decreases the containment level again and keeps it low until the pandemic almost ends after day 700.

Policy B on the efficient frontier results in an economic activity level of 85% and 515.3 lives lost per 100,000 individuals. In this case, the policy reacts less aggressively to the spread of the pandemic, that is, the decision maker waits longer to initiate a high level of containment, and the level is kept high for a shorter period of time. As a result, we observe a single but steeper peak in the pandemic.

When we move to point C on the efficient frontier, the level of economic activity increases to 90% and lives lost per 100,000 individuals increase to 577.4. In this case, as compared to policy B, the government initiates a high containment level earlier but keeps it for a shorter period, resulting in a slightly lower pandemic peak with a fatter and longer tail. These actions result in a higher level of economic activity at the expense of more lost lives.

When we compare policies A and C on the efficient frontier of the double-band containment policies, we observe that a 10-point increase in economic activity from 80% to 90% results in a 19.42% increase in lives lost under our base-case

TABLE 5 Absolute and percentage change in lives lost on the efficient frontier when the level of economic activity increases from 80% to 90% for varying levels of H and $\hat{\rho}_L/\rho_L$

		$\hat{\rho}_L/\rho_L$		
		1.2	**1.4**	**1.6**
H	0.00008	98.2 (21.85%)	102.6 (19.61%)	108.9 (19.16%)
	0.00010	93.9 (19.42%)	95.6 (18.19%)	99.2 (17.81%)
	0.00012	81.5 (17.69%)	87.5 (17.28%)	97.0 (16.53%)

parameter settings. This trade-off, however, naturally depends on the level of healthcare capacity and the rate of increase in lives lost when healthcare capacity is saturated, as measured by $\hat{\rho}_L/\rho_L$. Table 5 shows the impact of these two variables on lives lost when the level of economic activity increases from 80% to 90% on the efficient frontier.

To increase the level of economic activity, the government implements milder containment measures, which leads to more lives lost. As healthcare capacity increases, lives lost due to capacity saturation decreases, leading to a relatively lower death toll due to increased economic activity on the efficient frontier. Similarly, increasing the ratio $\hat{\rho}_L/\rho_L$ leads to more lives lost.

6.3 | Impact of disease parameters on Pareto-efficient policies

In this section, we examine the performance of Pareto-efficient solutions under a varying base infection rate (β_0) and recovery period ($1/\gamma$) as stated in Section 5.3, that is, $\beta_0 = \{0.2,\ 0.25,\ 0.3\}$ and $1/\gamma = \{7,\ 14,\ 21\}$.

In Figure 8, we consider the Pareto-efficient dynamic policies that achieve an 80% economic activity level.[14] Our base-case corresponds to the setting with $1/\gamma = 14$ and $\beta_0 = 0.25$. We observe that, when the base infection rate is low and recovery is fast ($\beta_0 = 0.2,\ 1/\gamma = 7$), adopting a mild containment regime prevents the disease from becoming a pandemic. Under a short recovery period ($1/\gamma = 7$), as the base infection rate increases, the Pareto-efficient policy leads to multiple small peaks when $\beta_0 = 0.25$ and 0.3. We observe a

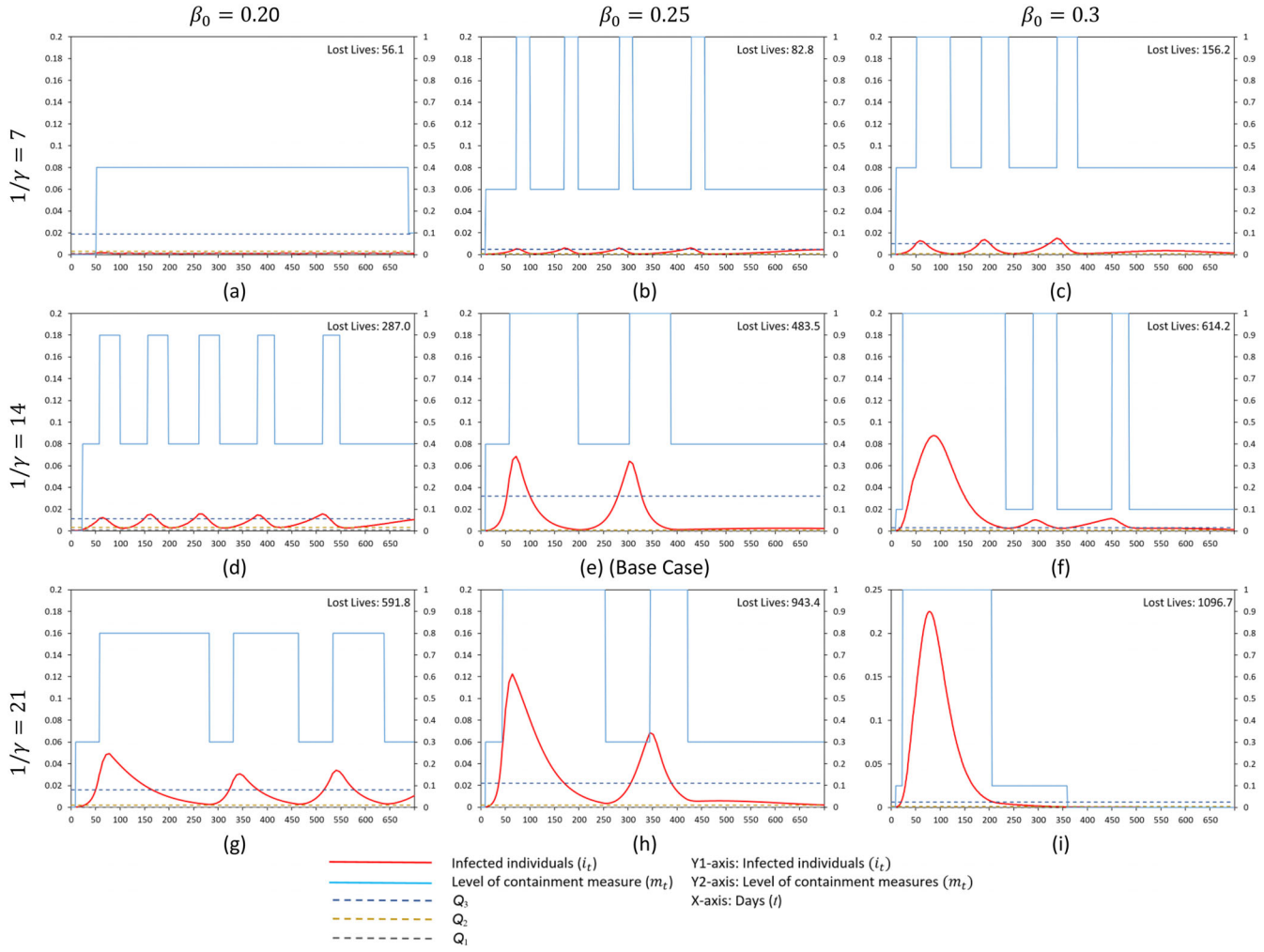

FIGURE 8 Impact of base infection rate β_0 and recovery period $1/\gamma$ on disease spread and Pareto-efficient dynamic containment policies at 80% economic activity level [Color figure can be viewed at wileyonlinelibrary.com]

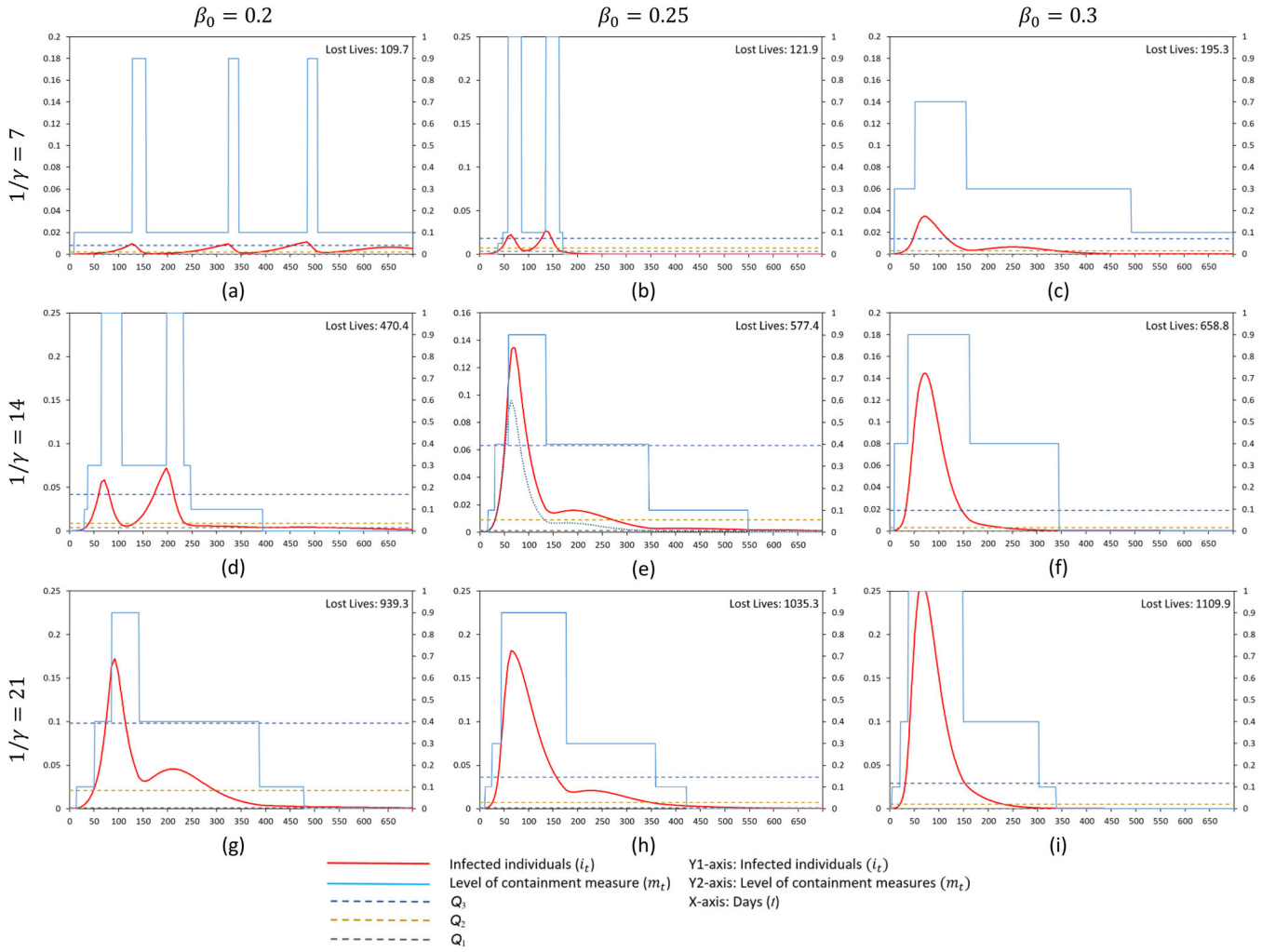

FIGURE 9 Impact of base infection rate β_0 and recovery period $1/\gamma$ on disease spread and Pareto-efficient dynamic containment policies at 90% economic activity level [Color figure can be viewed at wileyonlinelibrary.com]

similar pattern when the spread rate is low ($\beta_0 = 0.2$) and the recovery period is either medium or high ($1/\gamma = 14$ or 21). In general, for any given recovery period, higher infection rates result in fewer but steeper peaks over the course of pandemic. If the recovery is slow and the infection rate is high, then we typically observe a single steep peak, as the containment measures prove to be less effective in reducing the disease spread.

Figure 9 presents the same set of results for the Pareto-efficient dynamic policies that achieve a 90% economic activity level, that is, when the government targets a higher level of economic activity as compared to Figure 8. The results are qualitatively the same as the case in Figure 8, except that now we observe the government implements weak containment policies leading to fewer but steeper peaks in the pandemic. We repeated our analysis with other levels of economic activity and found that the insights above are robust with respect to the level of economic activity.

6.4 | Value of dynamic policies

In this section, we present the value of dynamic policies as compared to static policies under the Pareto-efficient set of decisions (Figure 10). In particular, for a given level of economic activity, we compare the minimum lives lost under dynamic and static policies. This analysis helps to enclose the economic and operational parameters under which dynamic policies provide significant gains (in terms of reduced lives lost) over static approaches. On the efficient frontier, we define the benefit of dynamic policy as: (lives lost under static policy − lives lost under dynamic policy).

We observe that the value of dynamic policies is highest when the level of economic activity is neither too high nor too low. This is because, under very high or low economic activity targets, there is little room for updating containment levels in response to changes in disease spread. We observe

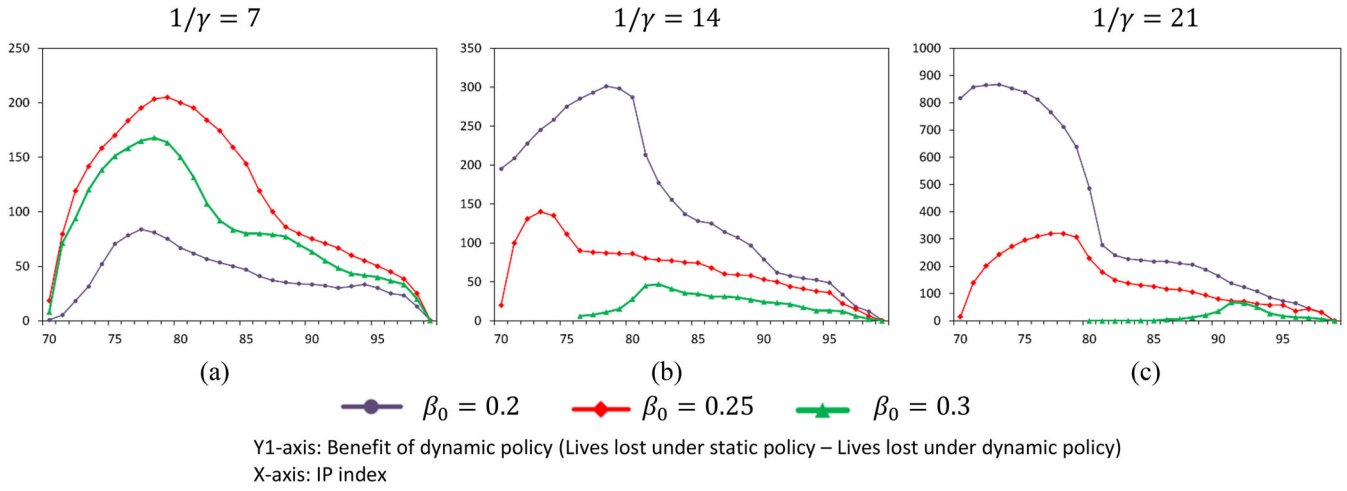

FIGURE 10 Value of dynamic policy for varying levels of economic activity, base infection rate β_0, and recovery period $1/\gamma$ [Color figure can be viewed at wileyonlinelibrary.com]

that the maximum benefit from a dynamic policy is obtained under low infection rate β_0 and high recovery period $1/\gamma$. As observed in Figures 8 and 9, under such disease patterns, the pandemic has the potential to cause many lives lost plus it is optimal to have multiple peaks, and hence flexibility becomes valuable.

7 | CONCLUSION

During a pandemic, governments face a key trade-off when imposing containment measures. Such measures can be effective in reducing disease spread and the load on the healthcare system, but they can also cause economic stall and social and political unrest, indirectly leading to reduced quality of life for the population. In this study, we examine this trade-off by providing a multiobjective decision model that incorporates both the economic and health implications of containment measures into a decision maker's objective function. We hope that our analysis will provide decision makers with valuable insights about when and how to implement containment measures during a pandemic.

We develop a decision-support framework for policymakers to determine the level of containment measures during a pandemic by integrating disease spread models with stochastic dynamic optimization models. We identify the Pareto-efficient set of containment policies under two common classes of control policies, namely static and dynamic. In general, as the recovery gets faster or the infection rate decreases, we observe more frequent but less steep peaks in the pandemic as the containment measures prove to be very effective in controlling the disease spread. However, when recovery is slow and the infection rate is high, then we typically observe a single steep peak because managing the spread of the disease with containment measures becomes very difficult. In addition, targeting a high level of economic activity is also likely to generate fewer but higher peaks in the pandemic.

The shape of the efficient frontier also reveals a key managerial insight about the sensitivity of governmental objectives to containment measures: Under low or high containment levels, the marginal impact of containment is low on economic activity but high on lives lost. However, for intermediate levels of containment measures, our results suggest that increasing (decreasing) containment level quickly reduces (increases) economic activity while resulting in little reduction (increase) in lives lost.

We also compare the performance of static and dynamic containment policies on the efficient frontier. We find that under very high or low economic activity targets, there is little room for updating containment levels in response to changes in disease spread, and hence there is little gain in using dynamic containment policies. Dynamic policies are particularly valuable when the disease parameters are likely to generate multiple peaks under a target economic activity level.

Our work can be extended in several directions. One possible extension could be considering an open population. Unlike the main assumption in the basic SIRD model, rather than requiring a closed population, one may include the possibility of incoming passengers through open and/or semiopen borders in the model. As another future work, an analysis could be conducted to incorporate the number of lives lost due to reduced economic activity and jobs lost driven by strict containment measures. Also, modeling uncertain vaccination effectiveness due to emerging new virus strains may be an interesting extension.

In addition to imposing disease containment measures to slow down disease spread, investing in healthcare capacity is an important dimension of pandemic management. In this study, we treat the healthcare capacity as a constant over time. While it is difficult to expand ICU capacity overnight, in medium and long term, acute care beds may be converted to ICUs or additional ICUs can be created. During the pandemic, governments have strived to increase healthcare

capacity either by building new and temporary hospitals (Lardieri, 2020; Zhu et al., 2020) or by converting acute care beds to ICUs (Panico, 2020) to meet the increasing demand for healthcare resources. A promising future research direction would be to consider integrating disease containment measures with healthcare capacity expansion decisions to improve the effectiveness of pandemic management.

ORCID

Masoud Shahmanzari https://orcid.org/0000-0003-2019-4490

ENDNOTES

[1] https://www.worldometers.info/coronavirus/.

[2] https://www.reuters.com/article/us-usa-economy-idUSKBN29D0J9.

[3] The IP index is available on a monthly basis, and hence it is preferable to use GDP data (available on a quarterly basis) to track the impact of pandemic and containment measures on economic activity.

[4] When characterizing an outbreak, R_0, known as the basic reproduction number, is frequently used. R_0 is a dimensionless ratio approximating the number of new infections caused by one infection. As an example, the seasonal flu is estimated to have an R_0 of approximately 1.3, while recent estimates for the R_0 of COVID-19 ranges from 1.4 to as high as 6.7 (usually early studies suggest larger numbers). Intuitively, any value smaller than 1 does not cause an outbreak. At any time t, this number is calculated by dividing the infection rate β_t by effective recovery rate γ.

[5] The dependence of $IP_t\left(\vec{m}_t; c_{IP}, \tilde{\epsilon}_{IP}\right)$ on IP_{t-1} is suppressed for notational brevity.

[6] In our notation, m_t is decided in period t, and it influences the infection number of the next period i_{t+1}, according to Equations (9), (12), and (13). For expositional simplicity, however, we denote $l_t(\vec{v}_t, \vec{m}_t; \tilde{\epsilon}_\beta)$ as the number of lives lost in period t, since m_t is determined in period t (although i_{t+1} is realized in the next period).

[7] This nonconvexity is driven by the evolution dynamics of pandemic diseases. When we present the models (6)–(14) in aggregate form, the decision variables are multiplied in constraints (8) and (9) leading to a nonconvex feasible region.

[8] http://www.nber.org/cycles/recession.html.

[9] https://www.imf.org/external/pubs/ft/weo/2019/02/weodata/index.aspx.

[10] Macroeconomic variables such as changes in labor and technology are not included in the model since these variables reflect structural changes in economies that take place over long periods of time, such as decades. In our analysis, even the whole sample period is less than 1 year.

[11] We have calculated these values based on the reported R_0 value given $\gamma = 1/14$.

[12] There are many novel variants of COVID-19 virus, including B.1.1.7 that was first detected in the United Kingdom. Volz et al. (2021) study the novel COVID-19 lineage, B.1.1.7 in the United Kingdom, and report that the new strain has 57% higher transmissibility on average. Their findings are compatible with another study conducted by researchers from Centre for the Mathematical Modelling of Infectious Diseases at the London School of Hygiene & Tropical Medicine who report that the recent variant B.1.1.7 is 50%–74% more transmissible (Davies et al., 2021). In our extended experiments in Appendix B in the Supporting Information, we investigate the impact of various mutation scenarios on our results.

[13] European Centre for Disease Prevention and Control (ECDC) has been regularly reporting and updating country response measures on COVID-19 since the start of the outbreak. According to their reports, earliest country-wide response measures were taken by Greece on February 28, 2020 (ECDC, 2021). Based on the ECDC data, we estimate $Q_{tr}^{\min}$ to be 0.00086%.

[14] Note that the upper bounds in Figures 8i and 9i are slightly higher than other graphs to fit the charts within the panel.

REFERENCES

Albi, G., Pareschi, L., & Zanella, M. (2021). Control with uncertain data of socially structured compartmental epidemic models. *Journal of Mathematical Biology*, *82*, https://doi.org/10.1007/s00285-021-01617-y

Ardabili, S. F., Mosavi, A., Ghamisi, P., Ferdinand, F., Varkonyi-Koczy, A. R., Reuter, U., Rabczuk, T., & Atkinson, P. M. (2020). Covid-19 outbreak prediction with machine learning. *Algorithms*, *13*(10), 249. https://doi.org/10.3390/a13100249

Boloori, A., & Saghafian, S. (2020). COVID-19: Health and economic impacts of societal intervention policies in the US. *SSRN*. http://doi.org/10.2139/ssrn.3681610

Chen, N., Gardner, L., & Rey, D. (2016). Bilevel optimization model for the development of real-time strategies to minimize *epidemic* spreading risk in air traffic networks. *Transportation Research Record*, *2569*(1), 62–69. https://doi.org/10.3141/2569-07

Davies, N. G., Abbott, S., Barnard, R. C., Jarvis, C. I., Kucharski, A. J., Munday, J., Pearson, C. A. B., Russell, T. W., Tully, D. C., Washburne, A. D., Wenseleers, T., Gimma, A., Waites, W., Wong, K. L. M., van Zandvoort, K., Silverman, J. D., CMMID COVID-19 Working Group, Diaz-Ordaz, K., Keogh, R.,… Edmunds, W. J. (2021). Estimated transmissibility and severity of novel SARS-CoV-2 variant of concern 202012/01 in England. *MedRxiv*. https://doi.org/10.1101/2020.12.24.20248822

Delen, D., Eryarsoy, E., & Davazdahemami, B. (2020). No place like home: Cross-national data analysis of the efficacy of social distancing during the COVID-19 pandemic. *JMIR Public Health and Surveillance*, *6*(2), e19862. https://doi.org/10.2196/19862

ECDC. (2021). *Data on country response measures to COVID*-19. https://www.ecdc.europa.eu/en/publications-data/download-data-response-measures-covid-19

Ehrgott, M. (2005). *Multicriteria optimization* (Vol. 491). Springer Science & Business Media.

Eryarsoy, E., & Shahmanzari, M., & Tanrisever, F. (2022). Models for government intervention during a pandemic. *European Journal of Operational Research*. https://doi.org/10.1016/j.ejor.2021.12.036

Ferguson, N., Laydon, D., Nedjati Gilani, G., Imai, N., Ainslie, K., Baguelin, M., Bhatia, S., Boonyasiri, A., Cucunubá, Z., Cuomo-Dannenburg, G., Dighe, A., Dorigatti, I., Fu, H., Gaythorpe, K., Green, W., Hamlet, A., Hinsley, W., Okell, L. C., van Elsland, S., … Ghani, A. (2020). Report 9: Impact of non-pharmaceutical interventions (NPIs) to reduce COVID19 mortality and healthcare demand. Imperial College London, London, UK.

Funk, S., Camacho, A., Kucharski, A. J., Eggo, R. M., & Edmunds, W. J. (2018). Real-time forecasting of infectious disease dynamics with a stochastic semi-mechanistic model. *Epidemics*, *22*, 56–61. https://doi.org/10.1016/j.epidem.2016.11.003

Ghaffarzadegan, N., & Rahmandad, H. (2020). Simulation-based estimation of the early spread of COVID-19 in Iran: Actual versus confirmed cases. *System Dynamics Review*, *36*(1), 101–129. https://doi.org/10.1002/sdr.1655

Giordano, G., Blanchini, F., Bruno, R., Colaneri, P., Di Filippo, A., Di Matteo, A., & Colaneri, M. (2020). Modelling the COVID-19 epidemic and implementation of population-wide interventions in Italy. *Nature Medicine*, *26*(6), 855–860. https://doi.org/10.1038/s41591-020-0883-7

Gormsen, N. J., & Koijen, R. S. (2020). Coronavirus: Impact on stock prices and growth expectations. *The Review of Asset Pricing Studies*, *10*(4), 574–597. https://doi.org/10.1093/rapstu/raaa013

Harris, J. (1987). QALYfying the value of life. *Journal of Medical Ethics*, *13*(3), 117–123. https://doi.org/10.1136/jme.13.3.117

Hethcote, H. W. (2000). The mathematics of infectious diseases. *SIAM Review*, *42*(4), 599–653. https://doi.org/10.1137/S0036144500371907

Keeling, M. J., & Rohani, P. (2011). *Modeling infectious diseases in humans and animals*. Princeton University Press.

Kyrychko, Y. N., Blyuss, K. B., & Brovchenko, I. (2020). Mathematical modelling of the dynamics and containment of COVID-19 in Ukraine. *Scientific Reports*, *10*(1), 1–11. https://doi.org/10.1038/s41598-020-76710-1

Lardieri, A. (2020, April 2). New York begins construction on more temporary hospitals as coronavirus spreads. *US News and World Report*.

Mrozek, J. R., & Taylor, L. O. (2002). What determines the value of life? A meta-analysis. *Journal of Policy analysis and Management*, *21*(2), 253–270. https://doi.org/10.1002/pam.10026

Murray, C. J. (1994). Quantifying the burden of disease: The technical basis for disability-adjusted life years. *Bulletin of the World Health Organization*, *72*, 429–445.

Ouardighi, F. E., Khmelnitsky, E., & Sethi, S. P. (2021). Epidemic control with endogenous treatment capability under popular discontent and social fatigue. *Production and Operations Management*. https://doi.org/10.1111/poms.13641

Ritchie, H., Mathieu, E., Rodés-Guirao, L., Appel, C., Giattino, C., Ortiz-Ospina, E., Hasell, J., Macdonald, B., Beltekian, D., & Roser, M. (2020). *Coronavirus pandemic* (*COVID*-19). Our World in Data. https://ourworldindata.org/coronavirus

University of Oxford. (2020). *Coronavirus government response tracker*. https://www.bsg.ox.ac.uk/research/research-projects/coronavirus-government-response-tracker

Panico, R. (2020, April 4). Bergen County hospital converts unused space into ICU beds for coronavirus patients. *NJ.com*.

Qiu, Y., Chen, X., & Shi, W. (2020). Impacts of social and economic factors on the transmission of coronavirus disease 2019 (COVID-19) in China. *Journal of Population Economics*, *33*, 1127–1172. https://doi.org/10.1007/s00148-020-00778-2

Roques, L., Klein, E., Papax, J., Sar, A., & Soubeyrand, S. (2020). Using early data to estimate the actual infection fatality ratio from COVID-19 in France. *MDPI Biology*, *9*(5), 97.

Rünstler, G., & Sédillot, F. (2003). Short-term estimates of euro area real GDP by means of monthly data. ECB Working Paper No. 276. European Central Bank (ECB).

Sanche, S., Lin, Y. T., Xu, C., Romero-Severson, E., Hengartner, N., & Ke, R. (2020). High contagiousness and rapid spread of severe acute respiratory syndrome coronavirus 2. *Emerging Infectious Diseases*, *26*(7), 1470–1477. https://doi.org/10.3201/eid2607.200282

Sene, N. (2020). SIR epidemic model with Mittag–Leffler fractional derivative. *Chaos, Solitons & Fractals*, *137*, 109833.

Singh, R., & Adhikari, R. (2020). Age-structured impact of social distancing on the COVID-19 epidemic in India. *arXiv preprint arXiv:*2003.12055.

Sugishita, Y., Kurita, J., Sugawara, T., & Ohkusa, Y. (2020). Effects of voluntary event cancellation and school closure as countermeasures against COVID-19 outbreak in Japan. *PLoS One*, *15*(12), e0239455. https://doi.org/10.1371/journal.pone.0239455

Tang, B., Wang, X., Li, Q., Bragazzi, N. L., Tang, S., Xiao, Y., & Wu, J. (2020). Estimation of the transmission risk of the 2019-nCoV and its implication for public health interventions. *Journal of Clinical Medicine*, *9*(2), 462. https://doi.org/10.3390/jcm9020462

Thunström, L., Newbold, S. C., Finnoff, D., Ashworth, M., & Shogren, J. F. (2020). The benefits and costs of using social distancing to flatten the curve for COVID-19. *Journal of Benefit-Cost Analysis*, *11*(2), 179–195. https://doi.org/10.1017/bca.2020.12

Trilla, A. (2020). One world, one health: The novel coronavirus COVID-19 epidemic. *Medicina Clínica* (*English Edition*), *154*(5), 175–177. https://doi.org/10.1016/j.medcle.2020.02.001

Viscusi, W. K., & Aldy, J. E. (2003). The value of a statistical life: A critical review of market estimates throughout the world. *Journal of Risk and Uncertainty*, *27*(1), 5–76. https://doi.org/10.1023/A:1025598106257

Volz, E., Mishra, S., Chand, M., Barrett, J. C., Johnson, R., Geidelberg, L., … & Ferguson, N. M. (2021). Assessing transmissibility of SARS-CoV-2 lineage B. 1.1. 7 in *England. Nature*, *593*(7858), 266–269.

Wearing, H. J., Rohani, P., & Keeling, M. J. (2005). Appropriate models for the management of infectious diseases. *PLoS Medicine*, *2*(7), e174. https://doi.org/10.1371/journal.pmed.0020174

Whitehead, S. J., & Ali, S. (2010). Health outcomes in economic evaluation: The QALY and utilities. *British Medical Bulletin*, *96*(1), 5–21. https://doi.org/10.1093/bmb/ldq033

Wu, J. T., Leung, K., & Leung, G. M. (2020). Nowcasting and forecasting the potential domestic and international spread of the 2019-nCoV outbreak originating in Wuhan, China: A modelling study. *Lancet*, *395*(10225), 689–697. https://doi.org/10.1016/S0140-6736(20)30260-9

Xie, G. (2020). A novel Monte Carlo simulation procedure for modelling COVID-19 spread over time. *Scientific Reports*, *10*(1), 1–9. https://doi.org/10.1038/s41598-020-70091-1

Zeckhauser, R., & Shepard, D. S. (1976). Where now for saving lives? *Law and Contemporary Problems*, *40*, 5–45.

Zhu, W., Wang, Y., Xiao, K., Zhang, H., Tian, Y., Clifford, S. P., Xu, J., & Huang, J. (2020). Establishing and managing a temporary coronavirus disease 2019 specialty hospital in Wuhan, China. *Anesthesiology*. https://doi.org/10.1097/ALN.0000000000003299

Zlojutro, A., Rey, D., & Gardner, L. (2019). A decision-support framework to optimize border control for global outbreak mitigation. *Scientific Reports*, *9*(1), 1–14. https://doi.org/10.1038/s41598-019-38665-w

SUPPORTING INFORMATION

Additional supporting information may be found in the online version of the article at the publisher's website.

How to cite this article: Shahmanzari, M., Tanrisever, F., Eryarsoy, E., & Şensoy, A. (2022). Managing disease containment measures during a pandemic. *Production and Operations Management*, 1–18. https://doi.org/10.1111/poms.13656